International Journal of Heat and Mass Transfer 54 (2011) 2560–2567

Contents lists available at ScienceDirect

International Journal of Heat and Mass Transfer

journal homepage: www.elsevier.com/locate/ijhmt

Molecular dynamics simulation of nanofluid's effective thermal conductivity in high-shear-rate Couette flow

Chengzhen Sun [a,b], Wen-Qiang Lu [a,*], Jie Liu [a], Bofeng Bai [b]

[a] College of Physical Sciences, Graduate University of Chinese Academy of Sciences, Beijing 100049, China
[b] State Key Laboratory of Multiphase Flow in Power Engineering, Xi'an Jiaotong University, Xi'an 710049, China

ARTICLE INFO

Article history:
Received 9 August 2010
Received in revised form 25 January 2011
Accepted 26 January 2011
Available online 23 February 2011

Keywords:
Effective thermal conductivity
Nanofluid
Couette flow
Modified Lees–Edwards periodic boundary
Microconvection

ABSTRACT

Effective thermal conductivity of Ar–Cu nanofluid in shear field is calculated by equilibrium molecular dynamics (EMD) simulation using Green–Kubo formula. The shear field is formed by imposing constant shear rate Couette flow with modified Lees–Edwards periodic boundary condition. The nanoparticle in the nanofluid in shear field rotates under the action of the velocity gradient. The rotation induces enhanced "microconvection" effect which is the main reason for the linear increase in the effective thermal conductivity of the shearing nanofluid with the shear rate increasing. The increase is more sharply with lower volume fraction of nanoparticle than with higher volume fraction, because the "microconvection" effect is weakened in the nanofluid with higher volume fraction of nanoparticle resulted by the slower nanoparticle rotation speed. The effective thermal conductivity obtained from the conventional correlation which is proposed for the flowing suspensions containing micro-sized particles are significantly lower than our numerical results. Moreover, the effect of nanoparticle volume fraction is more obvious in our numerical results. Therefore, the conventional correlation is not suitable when the sizes of the suspended particles are reduced to nanometers (nanofluid).

© 2011 Elsevier Ltd. All rights reserved.

1. Introduction

Nanofluid [1,2] containing nanometer sized particles or fibers suspended in the base fluid has received considerable attentions in last two decades, for its better heat transport performance than ordinary fluid containing micro-sized particles. Nanofluid shows great increase in thermal conductivity for a few additions of solid particles [3] and exhibits higher heat transfer coefficient in laminar flow [4,5] compared with the base fluid. Meanwhile, nanofluid is more stable and has acceptable viscosity and better wetting, spreading and adhesion behaviors on solid surface [6,7]. Among these behaviors, the high heat transport characteristic attracts extensive interests from scientists and more potential applications of nanofluid appear in many heat transfer areas.

Much work has been devoted to the investigation on the enhanced thermal properties of nanofluid and its enhancement mechanisms. Garg et al. [8] measured the thermal conductivity of copper nanoparticles in ethylene glycol and found that the increase in the thermal conductivity was twice the value predicted by the Maxwell effective medium theory. Sankar et al. [9] estimated the enhancement of the water–platinum nanofluid's thermal conductivity based on molecular dynamics simulation model and compared the results with the existing experimental results that indicated great enhancement in the thermal conductivity. Keblinski et al. [10] suggested four possible explanations for the anomalous enhancement in the thermal conductivity of nanofluid and showed that the key factor in the understanding of the thermal property of nanofluid is ballistic, rather than diffusive. In contrast, some scholars indicated that the increase in the thermal conductivity of nanofluid was not anomalous and the thermal conductivity was consistent with the classical effective medium theory. Buongiorno et al. [11] measured the thermal conductivity of various nanofluids using a variety of experimental approaches and concluded that no anomalous increase of thermal conductivity was observed and the experimental data were good agreement with the effective medium theory developed for dispersed particles. Vladkov and Barrat [12] simulated the thermal conductivity of nanofluid by molecular dynamics simulation and showed that in the absence of collective effects, the thermal conductivity of the nanofluid was well described by the classical Maxwell–Garnet equation mode.

Thermal property of nanofluid, a special kind of liquid–solid two-phase fluid, is related to not only the flow process, but also the heat transfer process. It is inadequate to replace the effective thermal conductivity of flowing nanofluid with its static thermal conductivity, which is often done before owing to the lack of relevant research on the effective thermal conductivity [13,14]. Shear

* Corresponding author. Tel./fax: +86 10 81717831.
E-mail address: luwq@gucas.ac.cn (W.-Q. Lu).

0017-9310/$ - see front matter © 2011 Elsevier Ltd. All rights reserved.
doi:10.1016/j.ijheatmasstransfer.2011.02.005

Nomenclature

r_{ij}	distance between atom i and atom j
r_{cut}	cutoff distance
N	total number of system atoms
V	system volume
T	system temperature
k_B	Boltzman constant
$\vec{J}$	heat current vector
t	time
Δt	time step length
$\vec{I}$	unit tensor
$\vec{v}$	velocity of atom
h	mean enthalpy
V_d	boundary velocity in x-direction
N_{fluid}	the total number of fluid atoms
m_i	mass of atom i
r_{zi}	z-direction component of position coordinate of atom i
$\vec{u}(r)$	local flow velocity
D_x	coordinate change in x-direction
L_x	width of simulation box in x-direction
r	radius of nanoparticle
$Vol\%$, c	volume fraction of nanoparticle/particles
Pe_p	Peclet number
d	diameter of particle
e	velocity gradient

Greek symbols

φ	LJ potential
ε	energy parameter
σ	length parameter
τ	nondimensional time
λ	thermal conductivity
γ	shear rate
ρ	liquid density
ω	rotation speed of nanoparticle
α	thermal diffusivity

Superscript

$*$	nondimensional quantities

Subscripts

s	solid nanoparticle
l	liquid base fluid
0	zero shear rate/static state
j, k	number of atoms
α, β	kind of atoms
m, n	time step
e	effective
f	suspending fluid

field is often encountered in industrial applications, in which the thermal property of two-phase fluid has been studied very early, both experimentally and theoretically [15–17]. The shear-induced enhanced microconvection is expected to be a common feature and one of the main reasons for the enhancement in the effective thermal conductivity in most disperse two-phase flow, such as bubbly flow, mist flow and solid–fluid slurry. Shin and Lee [18] experimentally measured the thermal conductivity of the suspension containing micrometer sized particles in shear flow fields and found that the thermal conductivity increased with the shear rate increasing and displayed asymptotic plateau values at high shear rate.

However, no work has been carried out on the thermal property of nanofluid in shear field, as far as our knowledge. Therefore, the purpose of our study is to investigate the influence of the flow shear rate on the effective thermal conductivity of the shearing nanofluid and probe the mechanisms of heat transfer enhancement. In this paper, the thermal conductivity of the nanofluid in shear field is calculated by molecular dynamics (MD) simulation method.

MD simulation is a computational method that solves Newton's equation of motion for a system of particles interacting with a given potential. As MD simulation directly and accurately calculates the movement of particles at atomic level, it can afford scientists and engineers ways to predict macroscopic properties based on generated primary data via statistical mechanicals. Meanwhile, there have been a number of methods devised to establish shear flow by MD simulation [19–21]. Of these, the homogeneous-shear (HS) method and the sliding-boundaries (SB) method have been proved to be popular. The SB method first employed by Ashurst and Hoover [19] was largely discarded due to the boundary effects, minimization of which needs to use large system size. While, it has been showed [22] that the results produced by the HS method were relatively insensitive to the system size above 200 system atoms. At the same time, in the homogeneous system all atoms perceive a similar environment because physical walls are eliminated.

Although there are many problems of the HS method such as high value of shear rate for small sample needed to drive the mass and heat flow, the shear viscosity has been computed widely with this method using Lees–Edwards [20] periodic-boundary to impose Couette flow on the sample by non-equilibrium molecular dynamics (NEMD) simulation. In contrast, in this paper the Couette flow is imposed to the nanofluid by equilibrium molecular dynamics (EMD) simulation with modified Lees–Edwards periodic boundary. In the EMD, transport properties are often calculated by Green–Kubo formula. It is the first attempt, to our knowledge, to calculate the thermal conductivity of shearing fluid in this way. It is expected that the calculation will be valuable both from methodological and engineering point of view.

2. Molecular dynamics simulation model

In this paper, the simulation system consists of liquid argon (Ar) base fluid and copper (Cu) nanoparticle. The widely accepted Lennard-Jones potential matches experimental data well for pure argon fluid and requires reasonable computation time. Although the most accurate potential for modeling copper atoms is embedded atom method (EAM) potential as it can take care of metallic bonding, the LJ potential also can predict well the qualitative trend of thermal conductivity enhancement [23]. In the simulation, the interatomic interactions between base fluid argon atoms, solid copper atoms, interactions between argon atoms and copper atoms are all modeled by the well-known Lennard-Jones (LJ) 12-6 potential [24],

$$\phi(r_{ij}) = \begin{cases} 4\varepsilon\left[\left(\frac{\sigma}{r_{ij}}\right)^{12} - \left(\frac{\sigma}{r_{ij}}\right)^{6}\right] & (r_{ij} < r_{cut}) \\ 0 & (r_{ij} \geqslant r_{cut}) \end{cases} \tag{1}$$

where r_{ij} is the distance between particles i and j, and σ and ε are the energy parameter which governs the strength of the interaction and the length scale, respectively. To improve the computational efficiency, only the neighbouring atoms within a certain cutoff ra-

dius (r_{cut}) are included in the force calculation because distant atoms have a negligible contribution. In this calculation, the cutoff distance r_{cut} is set to 2.5σ. For argon, the LJ parameters σ and ε are equal to 0.3405 nm and 1.670×10^{-21} J, respectively. For copper, the LJ parameters σ and ε are equal to 0.2338 nm and 65.625×10^{-21} J [23], respectively. To determine the parameters between argon atoms and copper atoms, the common Berthlot mixing rule is used [25]:

$$\sigma_{sl} = \frac{\sigma_{ss} + \sigma_{ll}}{2} \tag{2a}$$

$$\varepsilon_{sl} = \sqrt{\varepsilon_{ss}\varepsilon_{ll}} \tag{2b}$$

Therefore, σ and ε between argon and copper are 0.2871 nm and 10.469×10^{-21} J, respectively.

The system atoms are originally arranged in a regular faced-centred cubic (FCC) lattice. NVT ensemble is used in the simulation where total number of system atoms N, system volume V, and system temperature T are constant throughout the simulation. The tracks of the atom motion are obtained by integrating the motion equation with an effective Velocity-Verlet algorithm [26].

The EMD method can simulate transport coefficients, such as self-diffusion, thermal conductivity and shear viscosity, based on the linear response theory [27]. Thermal conductivity is obtained by integrating the heat current autocorrelation function (HCACF) through the Green–Kubo formula [28]

$$\lambda = \frac{1}{3Vk_BT^2}\int_0^\infty \langle \vec{J}(t)\cdot\vec{J}(0)\rangle dt \tag{3}$$

where λ is the thermal conductivity, V the system volume, T the system temperature, k_B the Boltzman constant, J the heat current vector, and the angular brackets denote the ensemble average or the average over time.

For a two-component system, the heat current is expressed as the constitution of the kinetic part, the collision part, and the potential part. Then, an extended form is used to calculate the heat current vector [29,30]

$$\begin{aligned}\vec{J} = &\sum_{\alpha=1}^{2}\sum_{j=1}^{N_\alpha}\frac{1}{2}m_\alpha v_{j\alpha}^2\vec{v}_{j\alpha} \\ &-\frac{1}{2}\sum_{\alpha=1}^{2}\sum_{\beta=1}^{2}\sum_{j=1}^{N_\alpha}\sum_{\substack{k=1\\k\neq j}}^{N_\beta}\left[r_{j\alpha k\beta}\frac{\partial\phi(r_{j\alpha k\beta})}{\partial r_{j\alpha k\beta}} - \phi(r_{j\alpha k\beta})\vec{I}\right]\vec{v}_{j\alpha} \\ &-\sum_{\alpha=1}^{2}h_\alpha\sum_{j=1}^{N_\alpha}\vec{v}_{j\alpha}\end{aligned} \tag{4}$$

where the subscripts j, k are the number of atoms, and α, β denote two different kinds of atoms. N_α and N_β are the number of atoms of α and β, respectively. $\vec{v}_{j\alpha}$ is the velocity of an atom j of α, h_α stands for the mean enthalpy per atom of α, and $\vec{I}$ is the unit tensor. The mean enthalpy is calculated as the sum of the average kinetic energy, potential energy, and virial terms per atom of each species [24]. For a single-component system, the last term of Eq. (4) equals zero.

Since the simulation is performed for discrete time steps, Eq. (3) for the calculation of thermal conductivity is written as below form.

$$\lambda(t_M) = \frac{\Delta t}{3k_BVT^2}\sum_{m=1}^{M}\frac{1}{N-m}\sum_{n=1}^{N-m}(\vec{J}(\vec{m+n})\cdot\vec{J}(\vec{n})) \tag{5}$$

where t_M is given by $M\,\Delta t$ and $\vec{J}(\vec{m+n})$ is the heat current vector at MD time step $m+n$. The average heat current vector over time is known as heat current autocorrelation function (HCACF).

In the model, the simulation box is considered as being embedded in a fluid which has a constant velocity gradient in the z-direction. Periodic boundary condition is imposed in the x–y plane, while modified Lees–Edwards periodic boundary condition, which will be illustrated in the next section, is applied in the z-direction to produce a constant shear rate Couette flow in the x-direction. The shear rate γ equals the velocity gradient $\gamma = \partial V_x/\partial z$. As an input parameter, the nondimensional shear rate $\gamma^* = \gamma/(1/\tau)$, where τ is the nondimensional time $\tau = \sigma\sqrt{m/\varepsilon}$, varies from 0.0 to 1.3 in this paper for the investigation of the influence on the effective thermal conductivity of nanofluid. A typical simulation requires 1,500,000–1,600,000 MD steps. The initial 100,000 time steps are used to allow the system to reach the temperature equilibrium. After the equilibrium, an extra velocity is given to the base fluid atoms and the modified Lees–Edwards periodic boundary condition is applied to form a linear velocity profile. It is necessary to control the temperature artificially in order to achieve steady state. The most simple and intuitive velocity rescaling [26] method is used to control the temperature, which changes the velocities of atoms at t time by multiplying a factor determined by the instantaneous temperature and the reference temperature. In the presence of flow, any local flow must be subtracted from the velocities before the evaluation of the temperature, which is calculated from:

$$T = \frac{1}{3N_{fluid}k_B}\sum_{i=1}^{N_{fluid}} m_i[\vec{v}_i - \vec{u}(r_i)]^2 \tag{6}$$

where the local flow velocity profile is simply given by

$$\vec{u}(r) = (\gamma r_{zi}, 0, 0) \tag{7}$$

The time step in the simulation is chosen from 0.0001τ to 0.0005τ depending on the value of shear rate. For large shear rate, a small time step is applied. When the velocity profile keeps stable after about 500,000 time steps, the data are collected to calculate the thermal conductivity according to the Green–Kubo formula.

3. Modified Lees–Edwards periodic boundary

In the Lees–Edwards periodic boundary condition, the box under consideration is surrounded by cyclic images of itself as in the conventional periodic boundary condition. While the neighbouring cells in the z-direction are made to drift with a specified speed V_d in the x-direction with respect to the central cell. The upper neighbouring cell is replaced with V_d, at the same time the lower cell is replaced with $-V_d$.

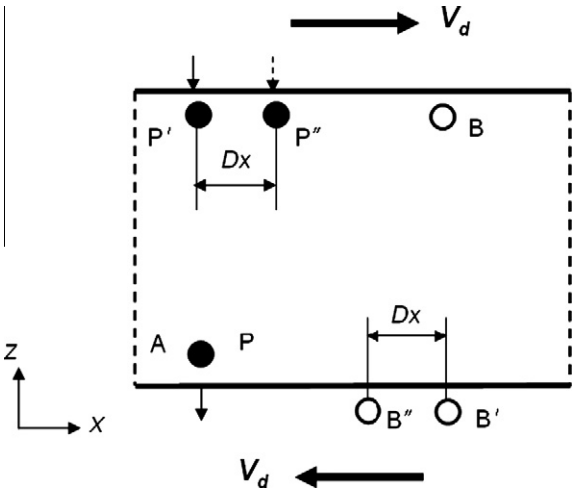

Fig. 1. A Couette flow set-up for constant shear rate and Lees–Edwards periodic boundary condition.

For the conventional periodic boundary condition, when an atom A leaves the simulation box at point P with velocity $\vec{V}$ from the lower boundary, as shown in Fig. 1, the atom will be reintroduced into the box at its symmetric point P' in the upper boundary with all three velocity components unaltered. While for the Lees–Edwards periodic boundary condition, the fluid atoms have a linear velocity profile and then the atom will be reintroduced into the box at point P'' with velocity $\vec{V}'$, where

$$\begin{aligned} V'_x &= V_x + 2V_d \\ V'_y &= V_y \\ V'_z &= V_z \end{aligned} \tag{8}$$

Meanwhile, there is a coordinate change D_x in the x-direction between the point P'' and the point P', which is given by

$$D_x = 2n_t V_d \Delta t - [2n_t V_d \Delta t / L_x] L_x \tag{9}$$

where n_t denotes the number of time step, and L_x is the width of the simulation box in the x-direction.

In the calculation of the interactions between boundary atoms, such as between atom A and atom B as shown in Fig. 1, the common method is Minimum Image Criterion [26], in which only the closer one with the atom A between the atom B and its image B′ is considered. In the Lees–Edwards periodic boundary condition, the image of atom B changes to B″, which have an offset value D_x along the velocity direction compared with B′.

However, when first applies the standard Lees–Edwards periodic boundary condition, the shear rate of the statistically obtained velocity profile of the pure fluid argon is not consistent with the imposed shear rate $\gamma^* = 0.5$, as shown in Fig. 2 (solid circles). At the same time, the region with linear velocity distribution is reduced to a small part of the central. The phenomenon is induced by the interactions separated by the z-boundaries, such as the interaction between the atom A and the image B″, because the velocity change between the atom B and its image B″ is not involved in the calculation of the interaction with Minimum Image Criterion. Since the nature of the interaction is not really reflected, the statistical average x-direction velocity of the atoms near the z-boundaries is lower than the velocity translated from the imposed shear rate. In order to obtain a constant shear rate velocity profile, the interaction must be modified. A straightforward modification is used in this paper, i.e. directly ignores the x-direction component of the interaction.

When the modified Lees–Edwards periodic boundary condition is applied to the same case of imposed shear rate $\gamma^* = 0.5$, linear velocity profile corresponding to the imposed shear rate is obtained as shown in Fig. 2 (solid squares). This demonstrates that our modification is effective to form constant high shear rate Couette flow.

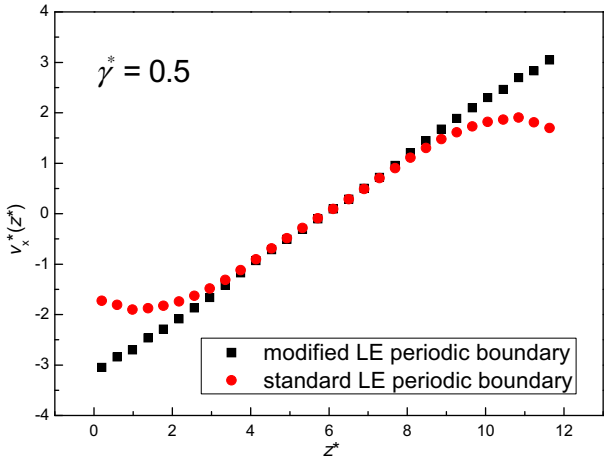

Fig. 2. Velocity profile of the pure fluid argon as imposing shear rate $\gamma^* = 0.5$.

4. Results and discussion

4.1. Validation of the simulation model

Prior to the calculation of the thermal conductivity of nanofluid, a validation of the computer code and the simulation model is conducted with the base fluid argon. It was observed by Sarkar and Selvam [23] that the thermal conductivity of argon base fluid is independent on the total number of system atoms above 500 atoms compared with 1372 atoms for nanofluid system. Hence, the thermal conductivity of liquid argon in the shear flow is calculated with 500 system atoms at its state point $T^* = 0.71$ and $\rho^* = 0.844(\sigma^{-3})$. Fig. 3 shows the HCACF diagrams and the thermal conductivity integrals of liquid argon with time step m (in Eq. (5)) for the shear rate $\gamma^* = 0.0$ (no shear flow) and $\gamma^* = 0.5$. It can be found that the thermal conductivity of the liquid argon in the shear flow nearly converges to the same value as that without shear flow. For a better understanding of the variation of the thermal conductivity with the shear rate, thermal conductivity of pure argon at various shear rates are further calculated.

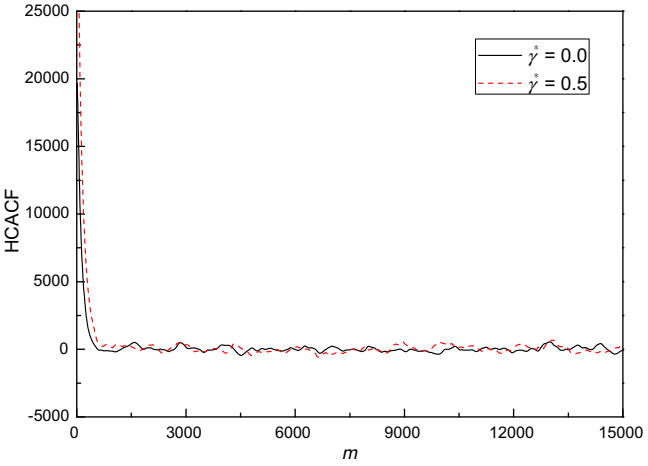

(a) HCACF

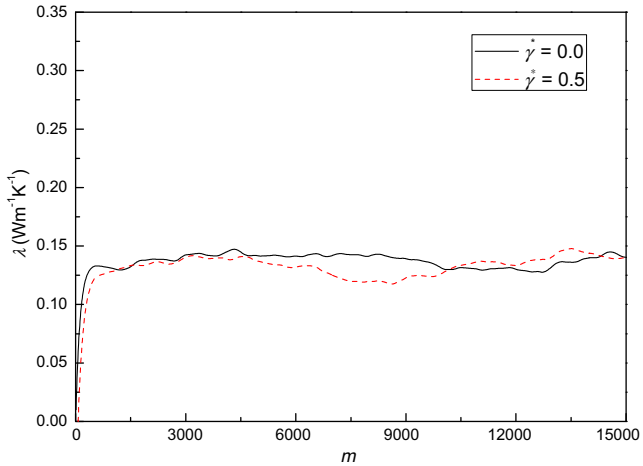

(b) Thermal conductivity

Fig. 3. HCACF and thermal conductivity of liquid argon as shear rate $\gamma^* = 0.0$ and $\gamma^* = 0.5$.

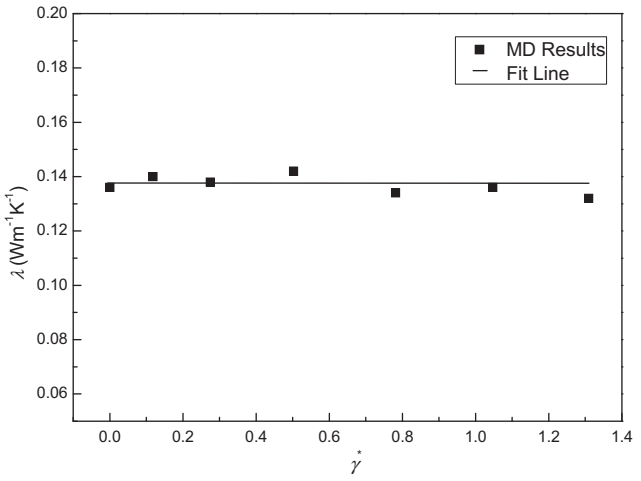

Fig. 4. Thermal conductivity of liquid argon as a function of flow shear rate.

Fig. 4 presents the thermal conductivity of argon vs. the nondimensional shear rate ranges from 0.0 to 1.3. The results demonstrate that there is no effect of the shear rate on the thermal conductivity and the constant value of the fitted line $\lambda = 0.138\ \mathrm{W\,m^{-1}\,K^{-1}}$ agrees well with the experimental value [23] $\lambda = 0.132\ \mathrm{W\,m^{-1}\,K^{-1}}$ at static state within 5%. The phenomenon is in accordance with the experimental conclusion by Sohn and Chen [17] and Shin and Lee [18] that the thermal conductivity of pure fluid has no dependence on the flow shear rate. Hence, our simulation results are proved to be accurate and the computer code and simulation model (including the modified Lees–Edwards periodic boundary condition) are validated.

4.2. Modeling the nanofluid and rotation of the nanoparticle

After the validation using pure argon, nanoparticle is suspended into the base fluid to form the nanofluid. The nanofluid system is modeled by replacing the same volume argon atoms with copper atoms according to the volume fraction of the nanoparticle (*Vol%*). The initial number of argon atoms is 1372, which is large enough to ensure that the results are independent from the number of atoms. Because the difference between the density of argon and copper is taken into account during the MD simulation, the solid nanoparticle is formed by carving sphere out of anther FCC lattice of copper atoms. Only a single solid nanoparticle is considered in the simulation. The temperature equilibrium structure of the nanofluid with *Vol%* = 1% appears as in Fig. 5.

Rotation of the copper nanoparticle is observed when the nanofluid is imposed a shear flow. A serial of figures which show the rotation of the nanoparticle for the shear rate $\gamma^* = 0.0$, 0.2 and 0.4 are provided in Table 1. When the flow reaches stable after 500,000 time step ($t = 0$), five copper atoms which located in the left of the *x*–*z* plane are selected to demonstrate the rotation. After 20 ps, for $\gamma^* = 0.0$ the nanoparticle nearly has no movement, while for $\gamma^* = 0.2$ and $\gamma^* = 0.4$ the nanoparticle appears a rotation along clockwise direction which can be observed from the location of the selected copper atoms. The higher the shear rate, the faster the rotation of the nanoparticle. It can be easily understood that the rotation is caused by the velocity difference between atoms of nanoparticle upper surface and lower surface, which is related to the flow shear rate.

The rotation of the nanoparticle can be quantified by evaluating the rotation speed ω skillfully through the tangential velocity of the copper nanoparticle. When the rotation is steady, for the leftmost surface atom, the *z*-direction velocity is approximately considered as the rotation tangential velocity. Thus, the rotation speed ω equals the *z*-direction velocity divided by the radius *r* of the nanoparticle. The rotation speeds of the nanoparticle in the

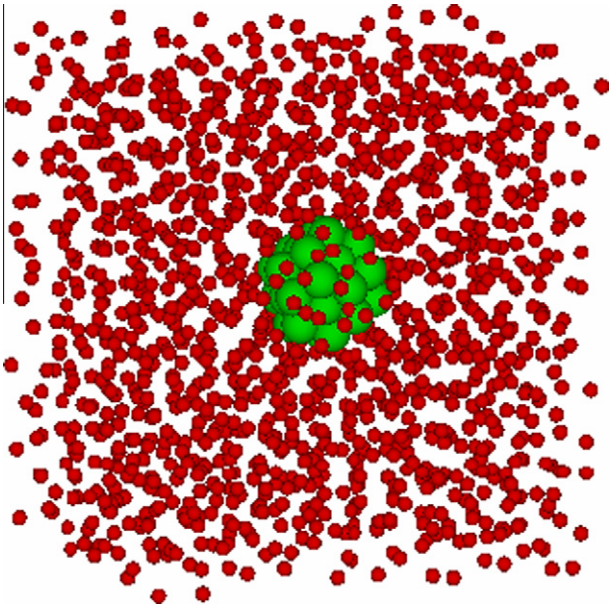

Fig. 5. Temperature equilibrium structure of the nanofluid with *Vol%* = 1% (green: copper nanoparticle; red: argon atoms). (For interpretation of the references to color in this figure legend, the reader is referred to the web version of this article.)

Table 1
Rotation of the nanoparticle in the *x*–*z* plane under different shear rates (green: copper nanoparticle; blue: selected copper atoms).

γ^*	t (ps)		
	0	20	40
0.0	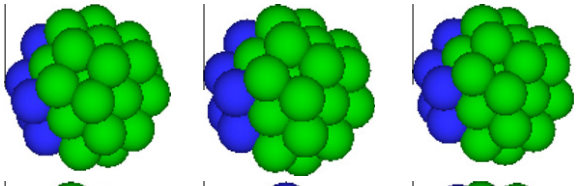		
0.2	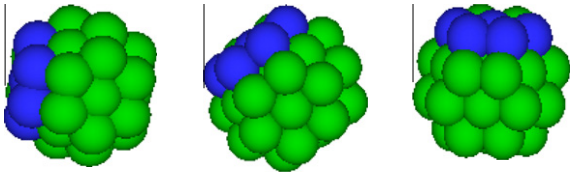		
0.4	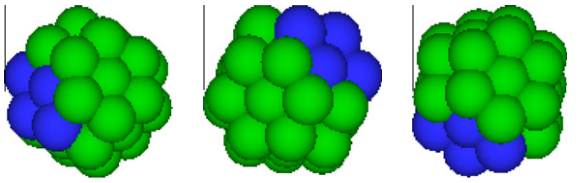		

Table 2
Rotation speed ω (rad/s) of the nanoparticle in the nanofluid with different volume fraction of nanoparticle for the shear rate $\gamma^* = 0.2$ and $\gamma^* = 0.4$.

γ^*	Vol%		
	1%	3%	5%
0.2	3.92×10^{10}	3.11×10^{10}	1.91×10^{10}
0.4	8.26×10^{10}	6.50×10^{10}	4.08×10^{10}

nanofluid with *Vol*% = 1%, 3% and 5% for shear rate $\gamma^* = 0.2$ and $\gamma^* = 0.4$ are shown in Table 2. For *Vol*% = 1%, 3% and 5%, the radius r of the nanoparticle are equal to 5.53×10^{-10} m, 7.72×10^{-10} m and 9.15×10^{-10} m, respectively. As can be seen from Table 2, the rotation speed increases significantly with increasing shear rate as found intuitively from Table 1. The rotation speed with a lower volume fraction at a certain shear rate is greater than that with a higher volume fraction, which is resulted by the bigger mass of nanoparticle for higher volume fraction.

4.3. Effect of nanoparticle volume fraction on the velocity profiles

When the nanoparticle is suspended into the base fluid, the velocity profile of the base fluid is influenced, as shown in Fig. 6. With the volume fraction of the nanoparticle increasing, the boundary values of the velocity profile are not altered, while the linear velocity distribution is affected. However, the change in the linear velocity distribution is slightly even though at the volume fraction of 5%.

4.4. Calculation of the thermal conductivity of nanofluid

Thermal conductivity of the nanofluid with *Vol*% = 1% for the shear rate $\gamma^* = 0.0$ and $\gamma^* = 0.3$ is calculated. The thermal conductivity of the nanofluid at shear rate $\gamma^* = 0.0$ is called zero-shear-rate thermal conductivity (λ_0). The HCACF diagrams and the thermal conductivity integrals with time step m are plotted in Fig. 7. The HCACF for $\gamma^* = 0.0$ decays to zero more rapidly and sharply, at the same time the HCACF for $\gamma^* = 0.3$ stays correlated more strongly and for a longer time. Accordingly, the thermal conductivity integral value for $\gamma^* = 0.3$ is remarkably higher than the zero-shear-rate thermal conductivity.

Thermal conductivity of the nanofluid at various shear rates is further calculated. Fig. 8 shows a relative thermal conductivity vs. nondimensional shear rate for *Vol*% = 1%, 3% and 5%. The relative thermal conductivity (λ_e/λ_0) is defined as the ratio of the effective thermal conductivity in shear flow to the zero-shear-rate thermal conductivity of nanofluid. For *Vol*% = 1%, 3% and 5%, 14, 38 and 68 of the argon atoms are replaced by 38, 164 and 266 copper atoms to model the nanofluid, respectively. Therefore, the total number of the atoms within the computational domain is 1396, 1498 and 1570, respectively. The zero-shear-rate thermal conductivity of the nanofluid with *Vol*% = 1%, 3% and 5% are equal to 0.159, 0.198 and 0.262 W m^{-1} K^{-1}, respectively.

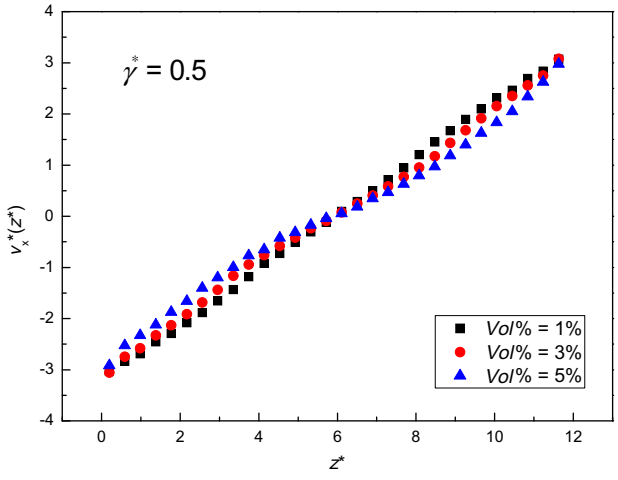

Fig. 6. Velocity profiles of the nanofluid with different nanoparticle volume fractions as imposed shear rate $\gamma^* = 0.5$.

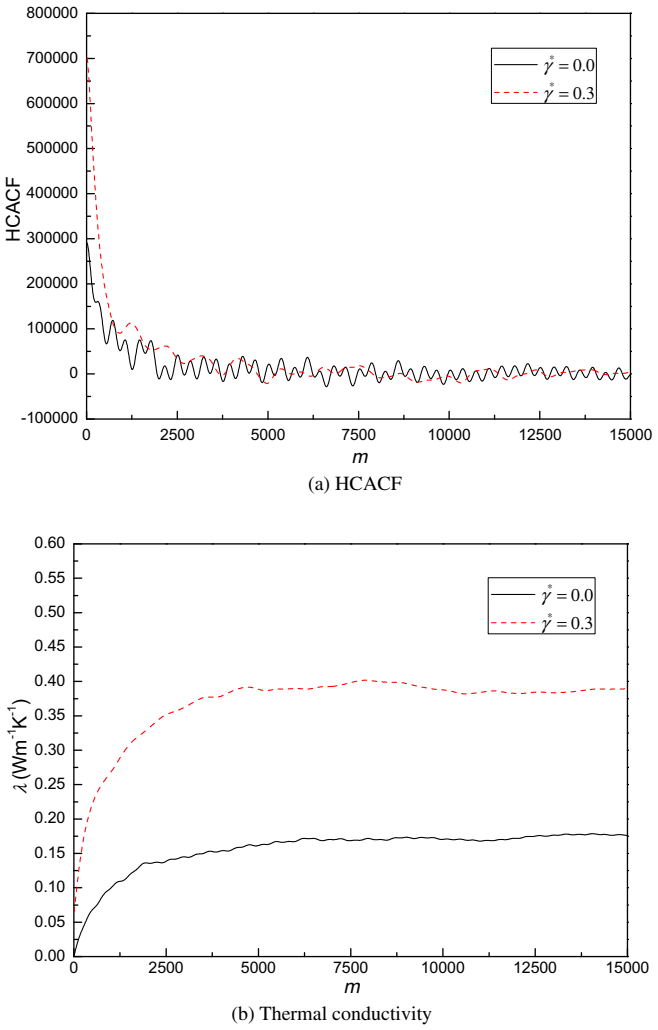

Fig. 7. HCACF and thermal conductivity of the nanofluid with *Vol*% = 1% as shear rate $\gamma^* = 0.0$ and $\gamma^* = 0.3$.

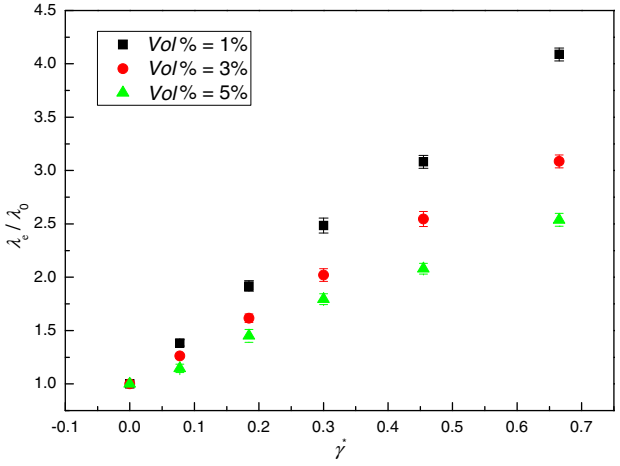

Fig. 8. Relative thermal conductivity vs. shear rate for the nanofluid with *Vol*% = 1%, 3% and 5%.

As seen from Fig. 8, the relative thermal conductivity at a certain volume fraction of nanoparticle increases nearly linearly as increases the nondimensional shear rate. Meanwhile, the volume

Table 3
The values of constant B and m.

	Low Pe_p	Moderate Pe_p (0.67–250)	Very high Pe_p
B	3.0	1.8	3.0
m	1.5	0.18	1/11

fraction effect is significant and the increase in the relative thermal conductivity at a lower volume fraction with respect to the shear rate is larger than that at a higher volume fraction. In other words, the shear rate effect on the effective thermal conductivity of shearing nanofluid with lower volume fraction is more obvious than with higher volume fraction.

As mentioned earlier, under a velocity gradient the nanoparticle behaves in an interesting manner: rotation. Thus, "microconvection" generated by the relative motion between the nanoparticle and the liquid fluid in the shearing nanofluid is stronger than that produced only by the Brownian motion of the nanoparticle in macroscopic static nanofluid. Therefore, thermal interactions between the rotating nanoparticle atoms and the base fluid atoms are stronger and accordingly the overall thermal transport is enhanced, in particular for high shear rate. At a higher volume fraction, the nanoparticle rotation speed slows down and the "microconvection" effect is weakened. Hence, the nanofluid with lower volume fraction has a greater increase in the thermal conductivity with the shear rate increasing than does with higher volume fraction.

According to Lin et al. [31], the shearing fluid structure become more aligned along the streamlines and thus become more orderly. However, the more aligned and orderly structure of the fluid atoms is not observed in the simulation from micro-structural point of view and the fluid structure with shear flow still acts like the temperature equilibrium structure as shown in Fig. 5. Therefore, it can be concluded that the shear flow has no effect on the structure of the fluid atoms and accordingly the orderly structure is not the reason for the enhancement in the thermal conductivity.

The effective thermal conductivity of flowing suspensions containing micro-sized particles was studied widely and Charunyakorn et al. [32] summarized a correlation according to the previous results.

$$\frac{\lambda_e}{\lambda_0} = 1 + BcPe_p^m \tag{10}$$

where λ_e is the effective thermal conductivity of the flowing suspension, λ_0 the thermal conductivity of the suspension at static state, c the volume fraction of the particles, and B and m are constants which are listed in Table 3, Pe_p is the particle Peclet number

$$Pe_p = \frac{ed^2}{\alpha_f} \tag{11}$$

where e is the velocity gradient, d the particle diameter, and α_f is the thermal diffusivity of the suspending fluid.

For the nanofluid with $Vol\%$ = 1%, 3% and 5%, the effective thermal conductivity is calculated by the conventional correlation equation (10) and the results are compared with our numerical results, as shown in Fig. 9. The results obtained from the conventional correlation are significantly lower than our numerical results, which mean that the effective thermal conductivity of the flowing nanofluid is seriously underestimated in Eq. (10). Furthermore, the volume fraction effect is more obvious in our numerical results. Therefore, the conventional correlation proposed for the suspensions containing micro-sized particles is not suitable as the sizes of the suspended particles reduced to nanometers (nanofluid) and a new correlation is expected.

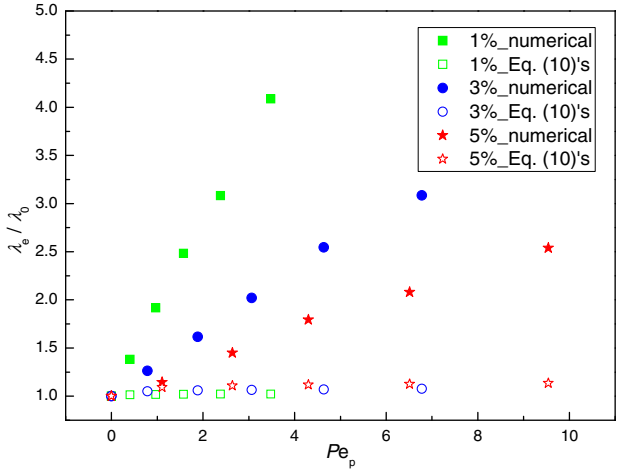

Fig. 9. Relative thermal conductivity compared between correlation results and our numerical results for the nanofluid with $Vol\%$ = 1%, 3% and 5%.

5. Conclusion

In this paper, the thermal conductivity of the argon-based nanofluid suspending copper nanoparticles in shear field is calculated by EMD simulation using Green–Kubo formula. The modified Lees–Edwards periods boundary condition is imposed to form Couette flow with constant shear rate.

In the shear field, the nanoparticle behaves in an interesting manner: rotation along clockwise direction in the x–z plane. The higher the shear rate, the faster the rotation of the nanoparticle. The rotation speed ω is greater with lower volume fraction of nanoparticle than that with higher volume fraction.

The relative thermal conductivity λ_e/λ_0 increases linearly as increases the flow shear rate for the enhanced "microconvection" effect resulted by the rotation of nanoparticle. The increase in the relative thermal conductivity at a lower volume fraction with respect to the shear rate is larger than that at a higher volume fraction, which is related to the slowed down rotation speed for the higher volume fraction of nanoparticle. This paper further point out that the shear flow has no effect on the fluid structure and orderly fluid structure is not the reason for the enhancement in the thermal conductivity of shearing nanofliud.

The effective thermal conductivity obtained from the conventional correlation equation (10) proposed for the flowing suspensions containing micro-sized particles is significantly lower than our numerical results. Furthermore, the volume fraction effect is more obvious in our numerical results. Hence, the conventional correlation is not suitable when the sizes of the suspended particles are reduced to nanometers (nanofluid).

Further research is needed to make a thorough probe into the thermal conductivity enhancement mechanisms of the nanofluid in shear field, especially from the microscopic point of view. At the same time, the influences of nanoparticle diameter, system temperature, etc. on the thermal conductivity enhancement need to be investigated and corresponding correlation try to be proposed.

Acknowledgements

This work is supported by the National Natural Science Foundation of China (Grant No. 50876111, Grant No. 50936006).

References

[1] J.A. Eastman, S.U.S. Choi, S. Li, W. Yu, L.J. Thompson, Anomalously increased effective thermal conductivities of ethylene glycol-base nanofluids containing copper nanoparticles, Appl. Phys. Lett. 78 (2001) 718–720.

[2] J.A. Eastman, S.R. Phillpot, S.U.S. Choi, P. Keblinski, Thermal transport in nanofluids, Annu. Rev. Mater. Res. 34 (2004) 219–246.

[3] S.K. Das, N. Putra, P. Thiesen, W. Roetzel, Temperature dependence of thermal conductivity enhancement for nanofluids, J. Heat Transfer 125 (2003) 567–574.

[4] Y.M. Xuan, Q. Li, Investigation on convective heat transfer and flow features of nanofluids, J. Heat Transfer 125 (2003) 151–155.

[5] Y.M. Xuan, Q. Li, Heat transfer enhancement of nanofluids, Int. J. Heat Fluid Flow 21 (2000) 58–64.

[6] D.T. Wasan, A.D. Nikolov, Spreading of nanofluids on solids, Nature 423 (2003) 156–159.

[7] M.K. Chaudhury, Spread the word about nanofluids, Nature 423 (2003) 131–132.

[8] J. Garg, B. Poudel, M. Chiesa, Enhanced thermal conductivity and viscosity of copper nanoparticles in ethylene glycol nanofluid, J. Appl. Phys. 103 (2008) 074301.

[9] N. Sankar, N. Mathew, C.B. Sobhan, Molecular dynamics modeling of thermal conductivity of thermal conductivity enhancement in metal nanoparticle suspensions, Int. Commun. Heat Mass Transfer 35 (2008) 867–872.

[10] P. Keblinski, S.R. Phillpot, S.U.S. Choi, J.A. Eastman, Mechanisms of heat flow in suspensions of nano-sized particles (nanofluids), Int. J. Heat Mass Transfer 45 (2002) 855–863.

[11] J. Buongiorno et al., A benchmark study on the thermal conductivity of nanofluids, J. Appl. Phys. 106 (2009) 094312.

[12] M. Vladkov, J. Barrat, Modeling transient absorption and thermal conductivity in a simple nanofluid, NanoLetters 6 (2006) 1224–1228.

[13] I.C. Bang, S.H. Chang, Boiling heat transfer performance and phenomena of Al2O3–water nanofluids from a plain surface in a pool, Int. J. Heat Mass Transfer 48 (2005) 2407–2419.

[14] H.E. Patel, S.K. Das, T. Sundararagan, A.S. Nair, B. George, T. Pradeep, Thermal conductivities of naked and monolayer protected metal nanoparticle based nanofluids: manifestation of anomalous enhancement and chemical effects, Appl. Phys. Lett. 83 (2003) 2931.

[15] L.G. Leal, On the effective conductivity of dilute suspension of spherical drops in the limit of low particle Peclet number, Chem. Eng. Commun. 1 (1973) 21–31.

[16] A. Nir, A. Acrivos, The effective thermal conductivity of sheared suspensions, J. Fluid Mech. 78 (1976) 3348.

[17] C.W. Sohn, M.M. Chen, Microconvective thermal conductivity in disperse two-phase mixture as observed in a laminar flow, J. Heat Transfer 103 (1981) 47–51.

[18] S. Shin, S.H. Lee, Thermal conductivity of suspension in shear flow fields, Int. J. Heat Mass Transfer 43 (2000) 4275–4284.

[19] W.T. Ashurst, W.G. Hoover, Dense-fluid shear viscosity via nonequilibrium molecular dynamics, Phys. Rev. A 11 (1975) 658.

[20] A.W. Lees, S.F. Edwards, The computer study of transport process under extreme conditions, J. Phys. 5 (1972) 1921–1929.

[21] D.J. Evans, G.P. Morriss, Nonlinear-response theory for steady planar Couette flow, Phys. Rev. A 30 (1984) 1528.

[22] D.J. Evans, G.P. Morriss, L.M. Hood, On the number dependence of viscosity in three dimensional fluids, Mol. Phys. 68 (1989) 637–646.

[23] S. Sarkar, R.P. Selvam, Molecular dynamics simulation of effective thermal conductivity and study of enhanced thermal transport mechanisms in nanofluids, J. Appl. Phys. 102 (2007) 074302.

[24] J.L. Xu, Z.Q. Zhou, Molecular dynamics simulation of liquid argon flow at platinum surfaces, Heat Mass Transfer 40 (2004) 859–869.

[25] G.Q. Chen, S.P. Chen, K. Chang, H.L. Su, Study of heat transfer of finned tube heat exchanger for cryogenic liquids, Vacuum & Cryogenics 13 (2007) 240–244.

[26] D. Frenkel, B. Smit, Understanding Molecular Simulation from Algorithms to Applications, Academic Press, Cornwall, UK, 1996.

[27] D.A. McQuarrie, Statistical Mechanics, University Science Books, Sausalito, 2000.

[28] W.Q. Lu, Q.M. Fan, Study for the particle's scale effect on some thermalphysical properties of nanofluids by a simplified molecular dynamics method, EABE (Innovative Numerical Methods for Micro and Nano Mechanics and Structures – Part II) 32 (2008) 282–289.

[29] C. Hoheisel, Theoretical Treatment of Liquids and Liquid Mixture, Elsevier, New York, 1993.

[30] J. Eapen, J. Li, S. Yip, Mechanism of thermal transport in dilute nanofluids, Phys. Rev. Lett. 98 (2007) 028302.

[31] S.X.Q. Lin, X.D. Chen, Z.D. Chen, B. Pratish, Shear rate dependent thermal conductivity measurement of two fruit juice concentrates, J. Food Eng. 57 (2003) 217–224.

[32] P. Charunyakorn, S. Sengupta, S.K. Roy, Forced convective heat transfer in microencapsulated phase change material slurries: flow in circular ducts, Int. J. Heat Mass Transfer 34 (1991) 819–833.